

Design and Analysis of Nozzle Exit Area for Science Technology Engineering and Mathematics (STEM) Based Solid Rocket Propellant

Muhammad Fadhli Hairi Abd Rahimi¹, Ahmad Hamdan Ariffin^{1*}

¹ *Research Center for Unmanned Vehicle (ReCUV), Faculty of Mechanical and Manufacturing Engineering, Universiti Tun Hussein Onn Malaysia, 86400 Parit Raja, MALAYSIA*

*Corresponding Author: ahmadh@uthm.edu.my
DOI: <https://doi.org/10.30880/paat.2025.05.02.002>

Article Info

Received: 4 July 2025
Accepted: 1 November 2025
Available online: 31 December 2025

Keywords

ANSYS Fluent, computational fluid dynamics, flow analysis

Abstract

The performance of a solid rocket propulsion system depends strongly on the geometric characteristics of its convergent-divergent (C-D) nozzle, particularly the exit area that determines the expansion of exhaust gases and the resulting thrust. This study investigates three C-D nozzle configurations with identical inlet and throat diameters using Computational Fluid Dynamics (CFD) simulations in ANSYS Fluent. Each nozzle was analyzed in terms of static pressure, temperature distribution, and velocity magnitude under the same operating conditions. The results indicate that all designs achieve choked flow at the throat, with peak velocities entering the supersonic regime. However, significant differences were observed downstream. Design B exhibits the most favorable flow characteristics, including a smooth pressure reduction of approximately 60–70% from inlet to throat, a uniform temperature decrease of about 25–30% across the divergent region, and the highest, most uniform exit velocity with minimal backflow. Designs A and C, in contrast, display irregular pressure recovery and non-uniform temperature and velocity gradients, indicating potential inefficiencies and localized separation. Overall, the findings confirm that nozzle contour geometry has a substantial effect on expansion efficiency, and the optimized configuration demonstrates strong potential for improving thrust and specific impulse in STEM solid rocket applications.

1. Introduction

The geometric configuration of a rocket nozzle plays a crucial role in determining the thrust and specific impulse of solid rocket propulsion systems. In a convergent-divergent (C-D) nozzle, the throat controls the mass flow rate, while the divergent section enables the exhaust gases to expand to supersonic speeds, directly influencing thrust performance [1]–[3]. For STEM-based solid rocket applications, understanding how variations in nozzle geometry modify flow behavior serves as an effective platform for demonstrating core aerospace engineering principles.

In this study, three nozzle configurations were developed with identical inlet and throat diameters but different geometric contours in the convergent and divergent sections. These variations are essential because the contour shape influences pressure gradients, shock formation, temperature distribution, and flow uniformity along the nozzle length [4], [5]. Literature indicates that curved diverging contours typically provide smoother flow acceleration and reduced separation compared to purely linear designs, resulting in improved exit flow conditions [6], [7].

Computational Fluid Dynamics (CFD) offers a powerful method to analyze these flow phenomena. Using ANSYS Fluent, high-resolution simulations can assess static pressure, temperature, and velocity distributions throughout the nozzle, revealing details about expansion behavior, boundary-layer interaction, and supersonic flow development [8], [9]. Through this simulation-based approach, learners gain a clear understanding of how nozzle geometry affects propulsion efficiency.

This research aims to design and analyze three C-D nozzle geometries for a STEM solid rocket propellant system. By comparing their CFD-predicted flow characteristics, the study identifies the design with the best overall performance, providing both practical engineering insights and a useful learning tool for STEM education environments.

2. Methodology

The methodology for this study follows a structured workflow consisting of nozzle design development, boundary condition definition, CFD setup, simulation execution, and comparative analysis.

2.1 Nozzle Design Parameters

Three nozzle designs were modeled with identical inlet diameter (20 mm), throat diameter (10 mm), and exit diameter (50 mm). Their geometric features—with varying combinations of linear or curved convergent and divergent contours—are shown in Fig. 2.1 and detailed in Table 2.1. The purpose of these variations is to evaluate how contour shape influences flow uniformity, supersonic expansion, and thermal distribution.

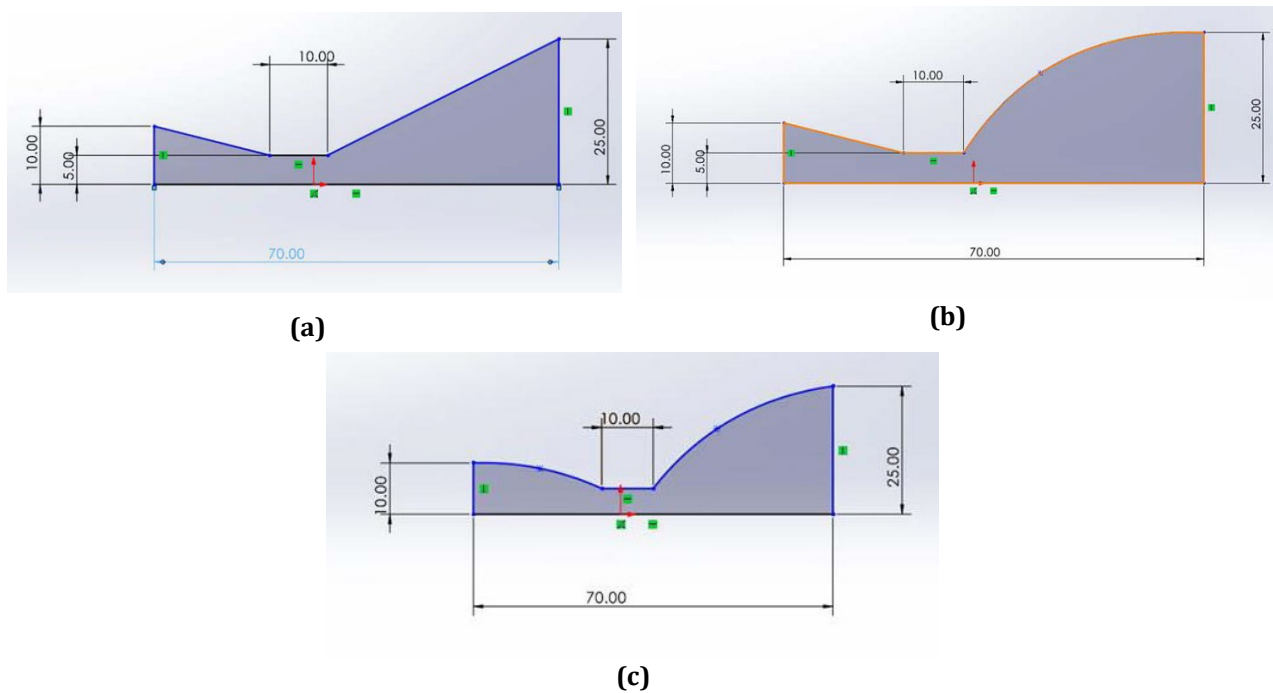


Fig. 1 Designs of C-D nozzle (a) Design A; (b) Design B; (c) Design C

Table 1 Design parameter for the bladeless wind turbine

Design	Inlet diameter (mm)	Throat diameter (mm)	Outlet diameter (mm)	Type
A	20	10	50	Divergence: linear Convergence: linear
B	20	10	50	Divergence: linear Convergence: curve
C	20	10	50	Divergence: curve Convergence: curve

2.2 Boundary Conditions

Defining appropriate boundary conditions is crucial, as they specify the behavior of the fluid at the domain boundaries and significantly influence the accuracy and stability of the simulation results. The boundary conditions used in the CFD simulation are listed in Table 2. These values are representative of typical gas conditions entering a small solid rocket nozzle.

Table 2 *Boundary conditions used in the CFD simulation*

Inlet total pressure (Pa)	Initial pressure (Pa)	Total inlet temperature (K)	Backflow total temperature (K)	Density (kg/m ³)	C _p
266904	225000	293	207.35	1.225	1006.43

2.3 CFD Setup Using ANSYS Fluent

The computational fluid dynamics analysis was performed with ANSYS Fluent, with the subsequent configuration: (i) Flow solver using density for compressible high-speed flows; (ii) The flow model is an ideal gas with the energy equation enabled. (iii) The mesh is fine-tuned at the throat to capture high pressure and velocity gradients. (iv) The simulation type is steady-state. (v) To guarantee convergence, iterate 4500 times per design. This modeling methodology adheres to established protocols in computational fluid dynamics research pertaining to supersonic nozzles [6], [8].

2.4 Performance Metrics and Post-Processing

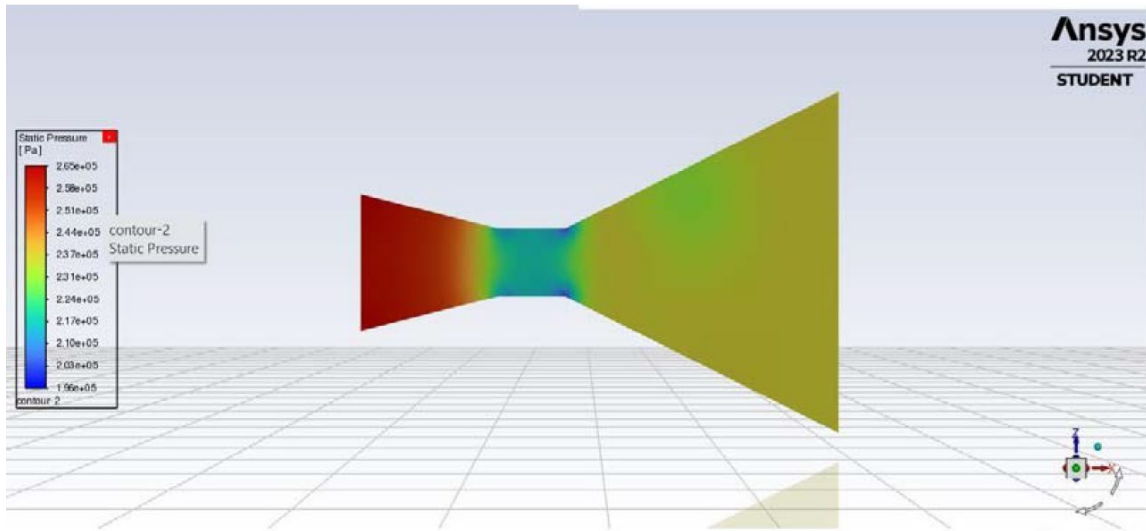
The subsequent flow parameters were derived from the CFD results: static pressure distribution, static temperature distribution, velocity magnitude, flow uniformity and separation behavior, and supersonic expansion characteristics. The assessment concentrates on determining which design produces the most effective expansion and minimal energy loss. The comparison was based on the smoothness of the pressure drop at the throat, temperature distribution uniformity, the presence of separation or backflow, supersonic expansion quality, and exit velocity magnitude.

3. Results and Discussion

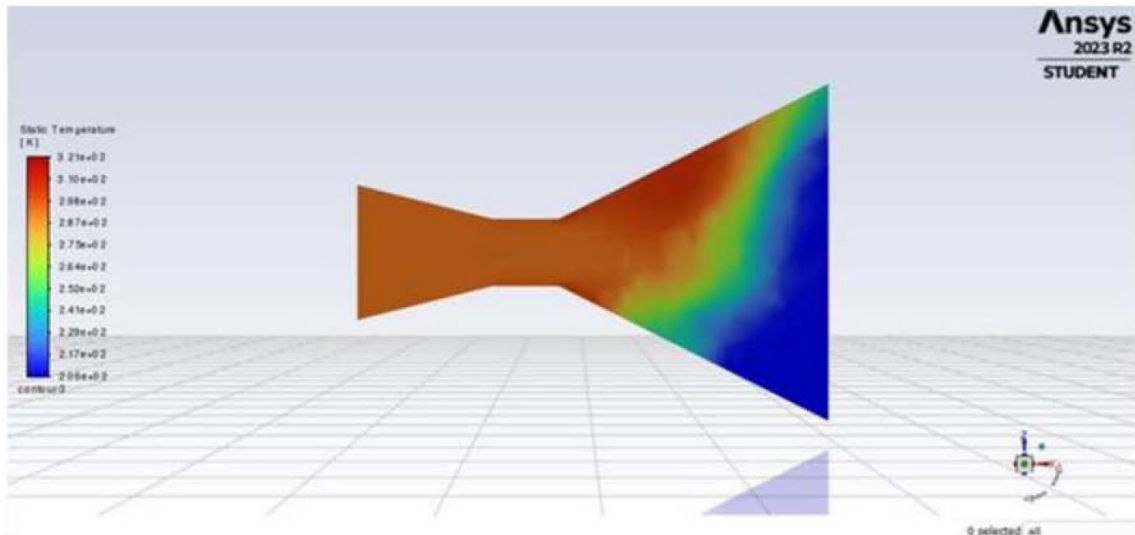
This section presents the findings obtained from the Computational Fluid Dynamics (CFD) simulations conducted on the three convergent-divergent (C-D) nozzle designs illustrated previously in Fig. 1(a)–(c) and described in Table 1. The flow behavior inside each nozzle was evaluated based on static pressure, static temperature, and velocity magnitude distributions.

3.1 Static Pressure Distribution

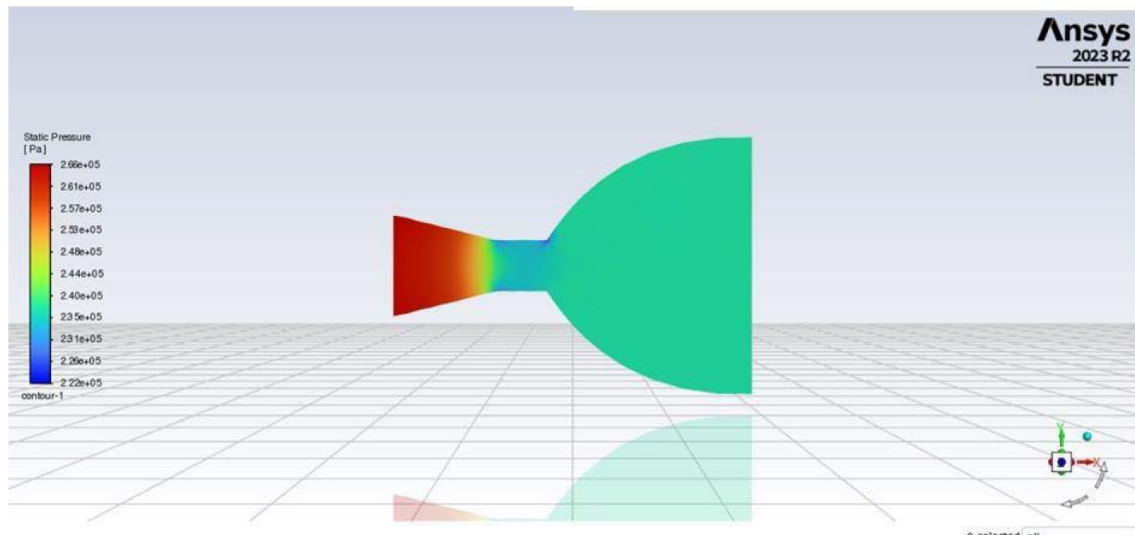
The static pressure contours for Designs A, B, and C are shown in Fig. 2. All three nozzles exhibit the expected rapid pressure drop at the throat, consistent with choked-flow conditions. However, the manner in which the pressure recovers in the divergent section varies significantly among the designs. Design A shows relatively high static pressure near the inlet, followed by a steep drop at the throat. However, the pressure distribution in the divergent region is uneven, indicating the possible formation of weak shock structures and localized flow separation. This behavior is likely influenced by the linear-linear contour combination used in this design (see Table 2.1). Design B, which incorporates a curved convergent and linear divergent profile, demonstrates the smoothest pressure transition. The pressure decreases steadily from inlet to throat—showing an approximate reduction of 60–70%—and continues to drop uniformly through the divergent section. This indicates efficient expansion and minimal flow disruption. The smoother contour shape in the converging region likely contributes to this performance. Design C exhibits the least favorable pressure characteristics. Although the initial and throat behavior is similar to the other designs, significant irregularities appear in the divergent section. These irregular pressure pockets may arise from flow instability linked to the fully curved contour configuration. Overall, Design B provides the most stable and efficient pressure distribution, aligning with established insights that curved convergent sections improve flow attachment and reduce separation.



(a)



(b)

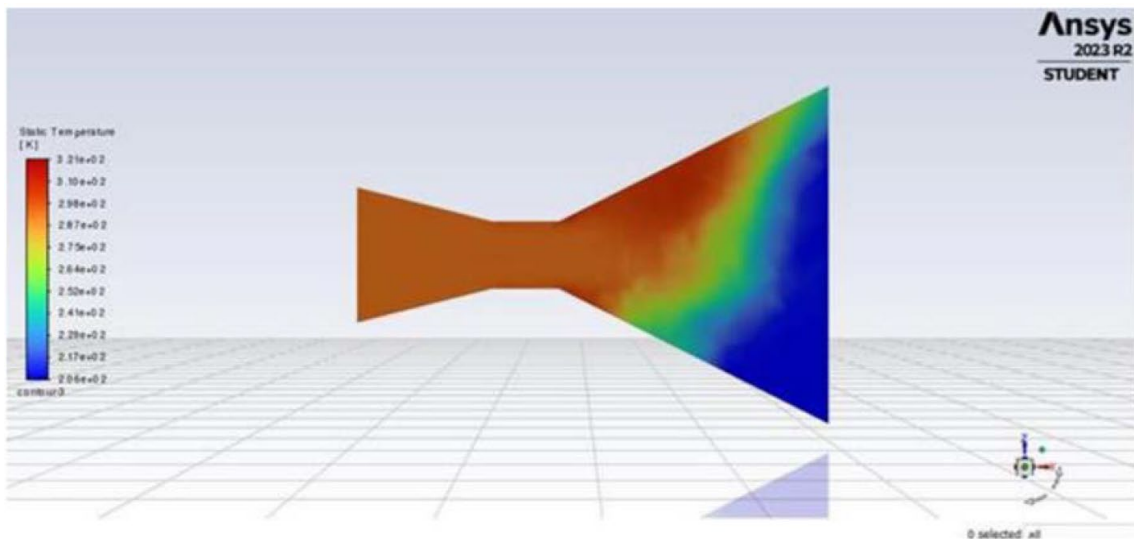


(c)

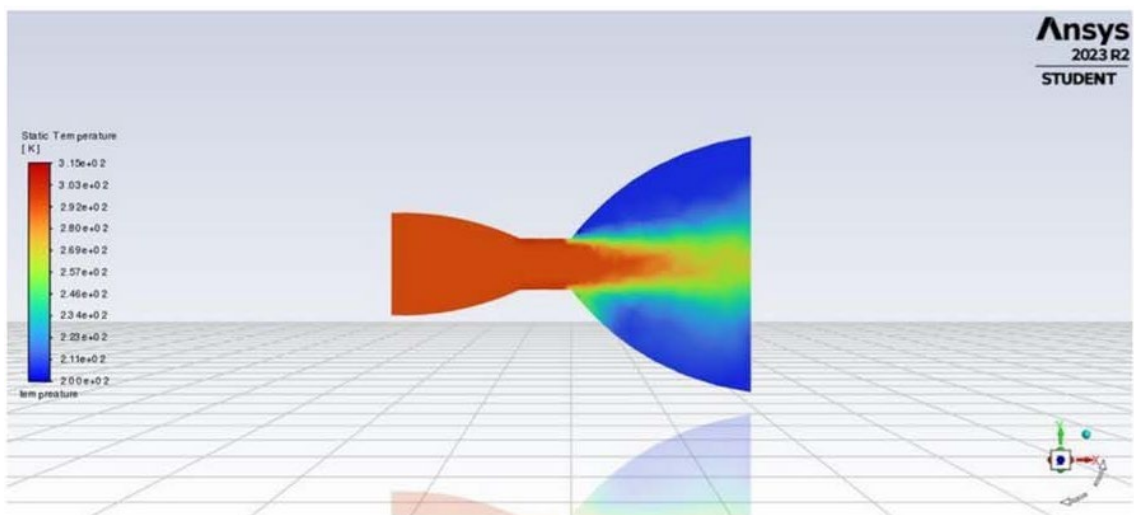
Fig. 2 Static pressure contour for C-D nozzle designs (a) Design A; (b) Design B; (c) Design C

3.2 Static Temperature Distribution

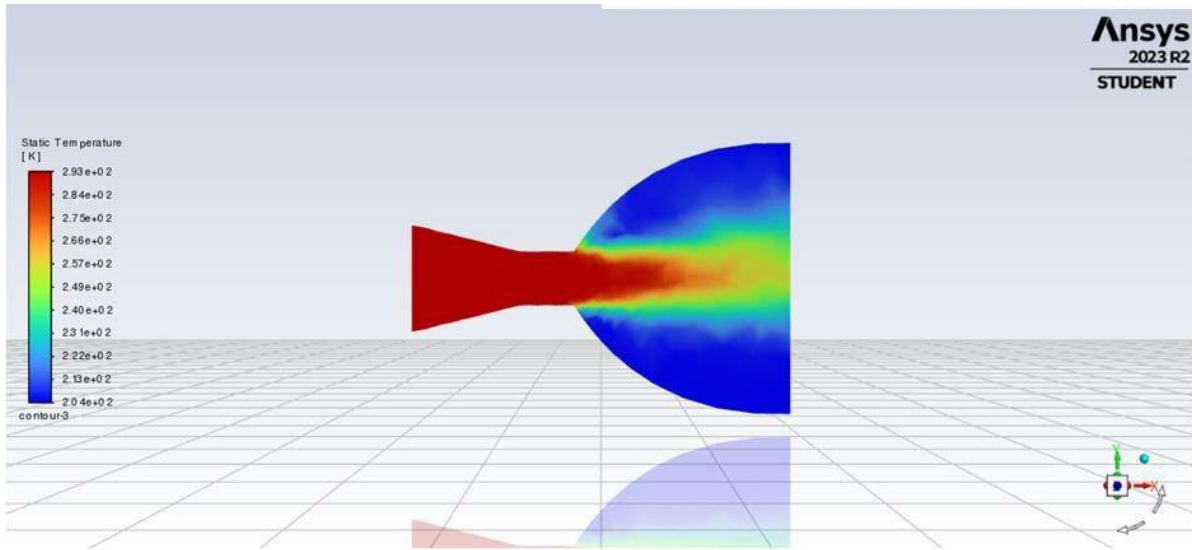
The static temperature results for the three nozzle designs are presented in Fig. 3. As expected, all designs show a decrease in static temperature as the flow accelerates from the convergent section to the divergent exit. However, the uniformity of this temperature reduction varies between designs. Design A displays high temperatures in the convergent region, but the divergent section shows noticeable non-uniformities. These temperature variations suggest uneven expansion and the presence of localized high-temperature zones, which may impose thermal stress on nozzle materials. Design B shows the most uniform temperature distribution. The temperature decreases steadily by approximately 25–30% from the convergent inlet to the exit plane, indicating effective energy conversion and smooth supersonic expansion. This uniformity is consistent with its smoother pressure profile. Design C experiences sharp temperature gradients, especially in the upper regions of the divergent nozzle. Such uneven thermal patterns typically indicate suboptimal expansion and can contribute to reduced mechanical and thermal efficiency. From a thermal-management perspective, Design B again demonstrates the most desirable behavior, with minimal hotspots and consistent temperature reduction across the nozzle length.



(a)



(b)

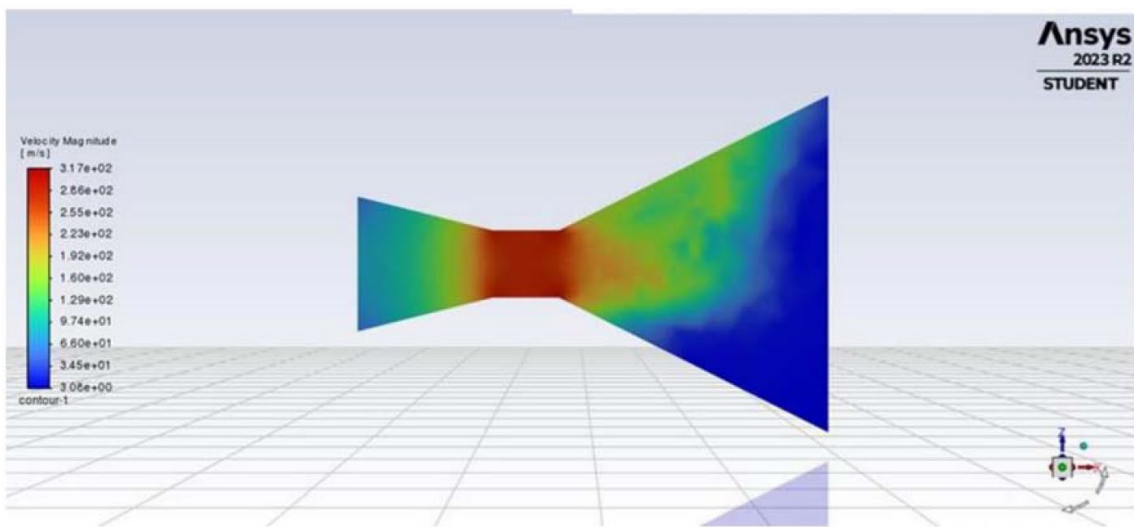


(c)

Fig. 3 Static temperature contour for C-D nozzle designs (a) Design A; (b) Design B; (c) Design C

3.3 Velocity Magnitude Distribution

Velocity magnitude contours for Designs A, B, and C are shown in Fig. 4. All designs achieve their highest velocity at the throat due to choked-flow conditions, consistent with theoretical expectations. Design A accelerates the flow successfully through the throat but develops non-uniform velocity regions in the divergent section. Some areas show signs of backflow or recirculation near the exit plane, which can decrease the effective thrust output. Design B demonstrates the most desirable velocity distribution. The flow accelerates smoothly through the throat into the divergent section, achieving uniform supersonic exit velocities. The absence of recirculation zones indicates well-aligned momentum flow, contributing to improved thrust generation. Design C shows inconsistent velocity patterns, with visible recirculation zones in the divergent region. These disturbances reduce exit-flow uniformity and may significantly affect thrust efficiency. These trends reinforce the superiority of Design B, which maintains the smoothest and most stable supersonic velocity profile throughout the nozzle.



(a)

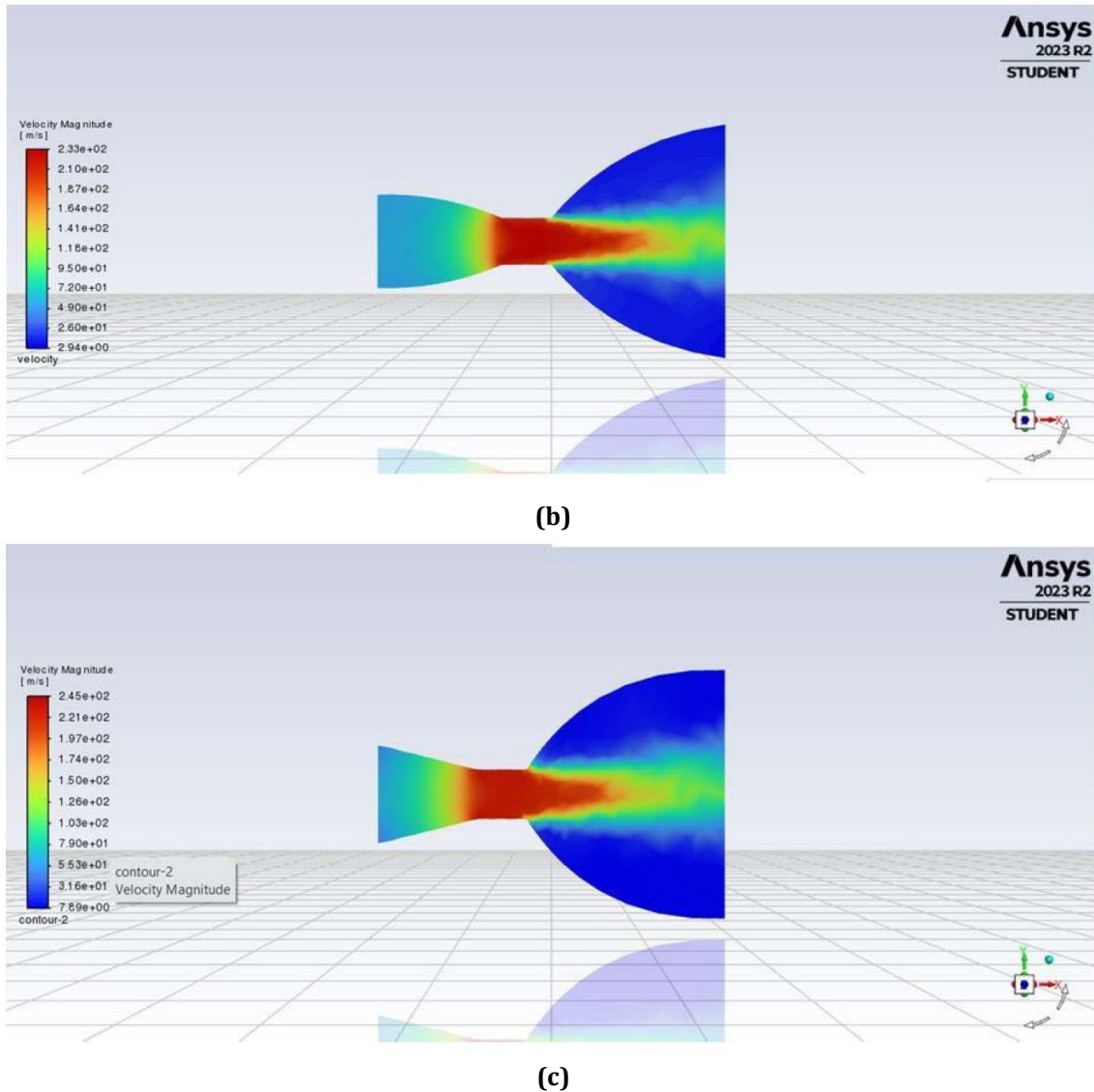


Fig. 4 Velocity magnitude contours for C-D nozzle designs (a) Design A (b) Design B (c) Design C

3.4 Comparative Performance Evaluation

When integrating the results from pressure, temperature, and velocity analyses, the relative performance of the three nozzle designs becomes clear. Design A provides acceptable flow acceleration but suffers from non-uniform pressure and temperature fields, as well as backflow near the exit. Design C exhibits the largest irregularities in flow behavior, with inconsistent pressure recovery, steep thermal gradients, and recirculation zones linked to its fully curved geometry. Design B repeatedly demonstrates the best flow stability, uniformity, and expansion efficiency, likely due to its balanced contour shape that combines a curved convergent section with a linear divergent exit. Design B's superior performance is consistent with previous studies suggesting that hybrid—curved-linear—contours provide advantageous flow characteristics by reducing separation risk while maintaining efficient supersonic expansion.

The geometric differences summarized in Table 1 explain much of the observed performance variation. Design B's curved convergent section improves flow alignment into the throat, reducing pressure losses and creating smoother temperature and velocity transitions. In contrast, the fully linear (Design A) and fully curved (Design C) profiles produce either abrupt transitions or overly sensitive flow behavior, leading to inefficiencies. The boundary conditions specified in Table 2 establish consistent inlet characteristics across all simulations, allowing differences observed in Figs. 2-4 to be attributed solely to geometric variations rather than operating conditions. Overall, the CFD visualizations clearly illustrate how modest changes in nozzle contour can significantly influence flow physics, thermal behavior, and momentum distribution.

4. Conclusions

This study investigated the flow characteristics of three convergent–divergent (C-D) nozzle designs for a STEM solid rocket propellant system using Computational Fluid Dynamics (CFD) simulations in ANSYS Fluent. Although all designs achieved the expected choked-flow condition at the throat and generated supersonic expansion in the divergent section, the results revealed clear differences in their overall aerodynamic performance.

Among the three configurations, Design B demonstrated the most favorable performance across all evaluation metrics. Its curved convergent and linear divergent profile produced a smooth and continuous pressure reduction from inlet to throat, followed by a stable expansion region with minimal flow disturbance. The temperature distribution in Design B was also more uniform, indicating efficient energy conversion and reduced thermal loading. Furthermore, the velocity magnitude contours showed highly uniform and stable supersonic exit flow, with no significant signs of backflow or recirculation. These characteristics collectively indicate better thrust potential and reduced aerodynamic losses compared to Designs A and C.

Design A, while functional, exhibited uneven pressure recovery and minor recirculation zones near the exit, which can compromise thrust efficiency. Design C experienced the greatest flow irregularities due to its fully curved geometry, resulting in inconsistent pressure trends, non-uniform temperature gradients, and velocity fluctuations within the divergent section.

Overall, the findings confirm that nozzle contour geometry plays a critical role in determining expansion efficiency, flow stability, and thrust performance. The hybrid contour approach used in Design B strikes an effective balance between smooth flow alignment in the convergent region and efficient supersonic acceleration in the divergent section. This makes Design B the most suitable candidate for further development in STEM solid rocket applications.

Future work may focus on experimental validation of the CFD results, exploration of additional contour variations, and investigation into material and thermal stresses to support full-scale implementation. The insights gained from this study not only enhance understanding of nozzle optimization but also provide a practical and visually intuitive learning platform for STEM education in propulsion and fluid dynamics.

Acknowledgement

The authors gratefully acknowledge the technical and administrative support from Universiti Tun Hussein Onn Malaysia (UTHM).

Conflict of Interest

There is no conflict of interest regarding the publication of the paper.

Author Contribution

The authors confirm their contribution to the paper, as follows: **study conception and design:** Muhammad Fadhli Hairi Abd Rahimi, Ahmad Hamdan Ariffin; **data collection:** Muhammad Fadhli Hairi Abd Rahimi; **analysis and interpretation of results:** Muhammad Fadhli Hairi Abd Rahimi, Ahmad Hamdan Ariffin; **draft manuscript preparation:** Muhammad Fadhli Hairi Abd Rahimi, Ahmad Hamdan Ariffin. All authors reviewed the results and approved the final version of the manuscript.

References

- [1] Zhang, Y., Cheng, M., Liu, X., Rong, G., Sheng, Z., Shen, D., Wu, K., & Wang, J. (2024). The influence of plug nozzle and Laval nozzle on the flow field and performance of non-premixed rotating detonation combustor. *Physics of Fluids*, 36(5). <https://doi.org/10.1063/5.0207508>
- [2] Zhang, L., Schickhardt, S., Merz, P., & Auffarth, G. U. (2024). Evaluation of Parameters and Nozzle Tip Damage after Clinical Use of Three Hydrophilic Intraocular Lens Injector Models. *Journal of Ophthalmology*, 2024, 1-8. <https://doi.org/10.1155/2024/2360368>
- [3] Zhang, G., Kim, H. D., & Jin, Y. Z. (2017). Analysis of choked two-phase flows of gas and particle in a C-D nozzle. *Theoretical and Applied Mechanics Letters*, 7(6), 331-338. <https://doi.org/10.1016/j.taml.2017.11.005>
- [4] Xue, Y., Bu, Y., Wang, S., Guan, B., & Wang, G. (2024). Numerical study on altitude-compensating mechanism of a permeable nozzle. *Journal of Physics: Conference Series*, 2746(1). <https://doi.org/10.1088/1742-6596/2746/1/012058>

- [5] Sharma, A. K., Vashishtha, A., Callaghan, D., Bakshi, S. R., Kamaraj, M., & Raghavendra, R. (2024). CFO Investigation of a Co-Flow Nozzle for Cold Spray Additive Manufacturing Applications. *Journal of Thermal Spray Technology*. <https://doi.org/10.1007/s11666-024-01764-w>
- [6] Seifelnasr, A., Si, X., & Xi, J. (2024). Effects of Nozzle Retraction Elimination on Spray Distribution in Middle-Posterior Turbinate Regions: A Comparative Study. *Pharmaceutics*, 16(5). <https://doi.org/10.3390/pharmaceutics16050683>
- [7] Panday, S., Rao, B. J., and Kumar, T. J. (2016). Computational Estimation of Flow through the C-D Supersonic Nozzle and Impulse Turbine Using CFD. *International Journal for Modern Trends in Science and Technology*, Vol 2, Issue 11, pp. 24-32. <https://www.researchgate.net/publication/328879237>
- [8] Peng, W., Ma, Y., Li, B., Wang, X., Peng, P., & Wang, J. (2024). Flow Field Simulation and Nozzle Parameter Optimization of Rust Removal Robot Based on High-Pressure Water Jet Technology. *Journal of Physics: Conference Series*, 2729(1). <https://doi.org/10.1088/1742-6596/2729/1/012006>
- [9] Munday, D., Gutmark, E., Liu, J., & Kailasanath, K. (2009). Flow structure of supersonic jets from conical C-D nozzles. *39th A/AA Fluid Dynamics Conference*. <https://doi.org/10.2514/6.2009-4005>